

---

# Neural Topographic Factor Analysis for fMRI Data

---

Eli Z. Sennesh\*  
esennesh@ccs.neu.edu

Zulqarnain Khan\*  
khanzu@ece.neu.edu

Jennifer Dy\*  
jdy@ece.neu.edu

Ajay B. Satpute\*  
a.satpute@northeastern.edu

J. Benjamin Hutchinson†  
bhutch@uoregon.edu

Jan-Willem van de Meent\*  
jwvdm@ccis.neu.edu

\*Northeastern University, †University of Oregon

## Abstract

Functional magnetic resonance imaging experiments produce gigabytes of high-dimensional spatio-temporal data for a small number of sampled participants and stimuli. Analyses of this data commonly average over all trials, ignoring variation among participants and stimuli. As a means of reasoning about this variation, we propose Neural Topographic Factor Analysis (NTFA), a deep generative model that parameterizes factors as functions of embeddings for participants and stimuli. We evaluate NTFA on a synthetically generated dataset, results from an in-house pilot study, and two publicly available datasets. We demonstrate that NTFA produces more accurate reconstructions with fewer parameters than related methods. Moreover, NTFA constitutes a first step towards reasoning about individual variation; learned embeddings uncover latent categories of stimuli, and partially separate latent groups of participants.

## 1 Introduction

Analyzing neuroimaging studies is both a large data problem and a small data problem. A single scanning run typically involves hundreds of full-brain scans that each contain tens of thousands of spatial locations (known as voxels). At the same time, neuroimaging studies tend to have limited statistical power. A typical study considers a cohort of 20-50 participants undergoing tens (or fewer) stimuli. A largely unsolved

challenge in this domain is to develop analysis methods that appropriately account for both the commonalities and variations among participants and stimuli effects, scale to tens of gigabytes of data, and reason about uncertainty to guard against overconfident predictions.

In this paper, we develop Neural Topographic Factor Analysis (NTFA), a family of models for analysis of spatio-temporal fMRI data that is suitable for reasoning about variations among participants and stimuli. NTFA extends Topographic Factor Analysis (TFA), an established method for fMRI analysis (Manning et al., 2014b), with a deep generative prior. This prior defines a distribution over embeddings (i.e. vectors of features) for each participant and stimulus, along with a conditional distribution over spatial and temporal factors, which is parameterized by a simple neural network. The result is a structured deep probabilistic model that can characterize variation among participants and stimuli, as well as interaction effects.

Our experiments compare NTFA to hierarchical topographic factor analysis (HTFA) (Manning et al., 2014a, 2018), a closely related method that employs a hierarchical Gaussian prior in lieu of our structured deep probabilistic model. We evaluate a total of four datasets, including data from a previously unpublished pilot study by the authors:

- As a basic validation of our model, we show that in a synthetic dataset simulated from clearly distinguishable clusters of participants and stimuli, inference recovers the true cluster structure.
- We present results for a pilot study on the neural basis of fear, carried out by the authors. In this study, participants are shown video clips of spiders, looming heights, and threatening social situations. The clips vary in how much fear they evoked, both within each category and across individuals. The stimulus embeddings learned by NTFA, which are fully unsupervised, group according to actual stim-

ulus categories. While the participant embeddings do not seem to predict the self-reported fear ratings, they do seem to uncover linear factors of variation in the latent space.

- Finally, we consider two publicly available datasets. In the first, participants listen to the narrative “Pie Man” (Simony et al., 2016). In the second, participants with major depressive disorder and controls listen to audio stimuli and music (Lepping et al., 2016). We find that NTFA yields more accurate reconstructions than HTFA, while employing a smaller number of trainable parameters.

Based on these findings, we believe that NTFA represents a meaningful step towards developing models that are able to characterize individual variation in an unsupervised manner. Concretely, the contributions of this paper can be summarized as follows:

- We develop NTFA (Section 3), a new model for analysis of fMRI data that infers embeddings for participants and stimuli that are shared across experiment trials. We perform inference using black-box variational methods that are implemented in Probabilistic Torch (Narayanaswamy et al., 2017).
- We show that NTFA achieves a lower reconstruction loss with fewer trainable parameters than HTFA, which represents of the state of the art.
- We demonstrate that embeddings, learned without supervision, correlate with experimental design variables and behavioral measures (Section 5). To our knowledge, NTFA is the first model able to characterize participants and stimuli in this way.

Figure 1 shows an overview of the proposed approach. Section 2 covers the related work in Factor Analysis for neuroimaging data, primarily HTFA which forms the basis for this work. Section 3 develops the NTFA model and Section 4 discusses experiments and results.

## 2 Background

Factor analysis methods are widely used to reduce the dimensionality of neuroimaging data. These methods decompose the fMRI signal for a trial  $Y \in \mathbb{R}^{T \times V}$  with  $T$  time points and  $V$  voxels into a product  $Y \simeq W \cdot F$  between a lower-rank matrix of weights  $W \in \mathbb{R}^{T \times K}$  and a lower-rank matrix of factors  $F \in \mathbb{R}^{K \times V}$ .  $K$  is chosen arbitrarily, and typically  $K \ll V$ . General-purpose methods that have been applied to fMRI data include Principal Component Analysis (PCA) (Abdi and Williams, 2010) and Independent Component Analysis (ICA) (Hyvärinen et al., 2001). A number of

methods have also been developed specifically for fMRI analysis, such as Hyper-Alignment (HA) (Haxby et al., 2011) and Topographic Latent Source Analysis (TLSA) (Gershman et al., 2011).

In this paper, we extend topographic factor analysis (Manning et al., 2014b) and Hierarchical Topographic Factor Analysis (Manning et al., 2014a, 2018), which represent the state of the art. TFA is a probabilistic factor analysis model that uses radial basis functions to define spatially smooth factors. HTFA itself extends TFA by drawing TFA’s model parameters from a Gaussian hyperprior shared across trials.

We will consider the task of modeling data that comprises  $N$  trials (i.e. continuous recordings) each of which contain  $T$  time points for voxels at  $V$  spatial positions. TFA defines a probabilistic model that approximates each trial  $Y_n \simeq W_n F_n$  as a product between a matrix of  $K$  time-varying weights  $W_n \in \mathbb{R}^{T \times K}$  and a matrix  $F_n \in \mathbb{R}^{K \times V}$  of  $K$  spatially-varying factors. To do so, TFA assumes that the data is noisily sampled from the inner product of the weights and factors matrices

$$Y_n \sim \mathcal{N}(W_n \cdot F_n, \sigma^Y). \quad (1)$$

TFA combines this likelihood  $p(Y_n | W_n, F_n)$  with a prior  $p(W_n, F_n)$ , which defines a probabilistic model  $p(Y_n, W_n, F_n)$ . TFA performs inference by approximating the posterior  $p(W_n, F_n | Y_n)$  with a variational distribution  $q_\lambda(F_n, W_n)$ , and optimizing its parameters.

TFA assumes means  $\mu_{n,k}^W$  and standard deviations  $\sigma_{n,k}^W$  for each factor’s weights over time, and defines a hierarchical Gaussian prior of the form

$$W_{n,t,k} \sim \mathcal{N}(\mu_{n,k}^W, \sigma_{n,k}^W), \quad \mu_{n,k}^W \sim p(\mu^W), \quad \sigma_{n,k}^W \sim p(\sigma^W).$$

To model the factors  $F_n$ , TFA employs a kernel function that ensures spatial smoothness of factor values  $F_{n,k,v}$  at similar voxel positions  $x_v^G \in \mathbb{R}^3$ . This kernel function  $\kappa$  is normally a radial basis function (RBF), which models each factor  $k \in K$  as a Gaussian with center at a spatial location  $x_{n,k}^F \in \mathbb{R}^3$ , whose width is determined by the kernel hyper-parameters  $\rho_{n,k}^F$ ,

$$F_{n,k,v} = \kappa(x_v^G, x_{n,k}^F; \rho_{n,k}^F), \quad (2)$$

with priors over both positions and widths,

$$x_{n,k}^F \sim p(x^F), \quad \rho_{n,k}^F \sim p(\rho^F). \quad (3)$$

Interpreting factor analysis probabilistically enables us to incorporate additional assumptions in order to capture variation and similarities between multiple sets of trials. HTFA (Manning et al., 2014a, 2018), introduces variables  $\bar{x}_k^F$  and  $\bar{\rho}_k^F$  representing each factor’s mean positions and widths across trials,

$$x_{n,k}^F \sim p(x_{n,k}^F | \bar{x}_k^F), \quad \bar{x}_k^F \sim p(\bar{x}^F), \quad (4)$$

$$\rho_{n,k}^F \sim p(\rho_{n,k}^F | \bar{\rho}_k^F), \quad \bar{\rho}_k^F \sim p(\bar{\rho}^F). \quad (5)$$

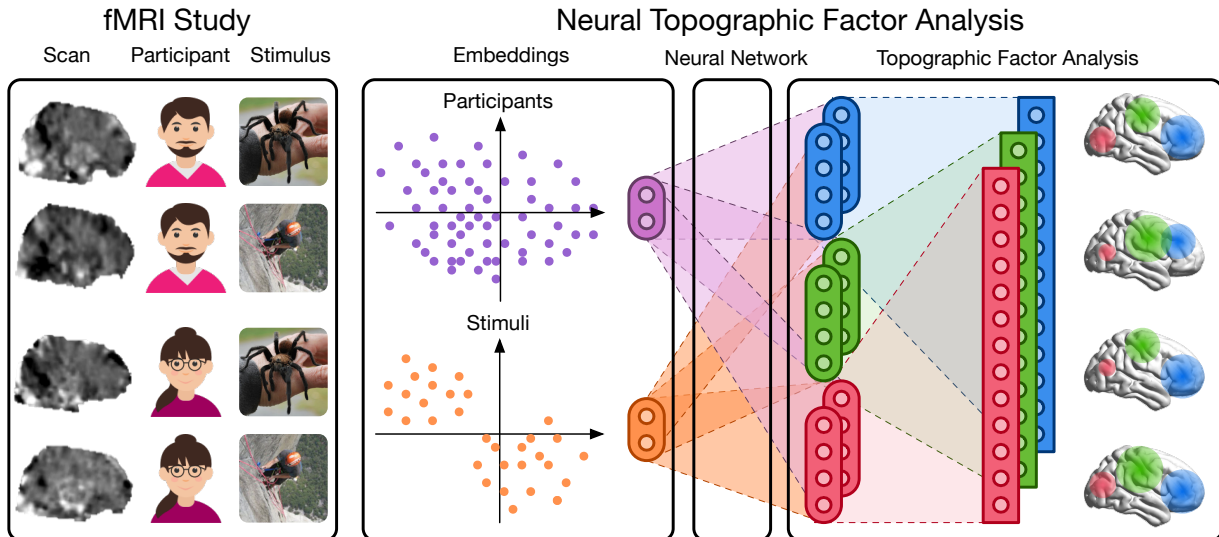


Figure 1: **Overview of Neural Topographic Factor Analysis (NTFA)**: We extend topographic factor analysis (TFA) (Manning et al., 2014b,a) to decompose the fMRI signal into Gaussian factors (shown in red, green and blue in the figure) that correspond to spatially and temporally related brain activity across individuals. A typical fMRI study consists of multiple trials of participants undergoing scans while experiencing different stimuli (or performing different tasks). In our generative model we represent these participants (purple) and stimuli (orange) with embedding vectors. A decoder network then predicts the location, size, and mean response of the Gaussian factors.

This prior is able to model multimodal responses to an extent, in the sense that factor positions and widths for individual trials are allowed to vary relative to a shared mean. However, the Gaussian hyperprior in HTFA assumes that neural responses across trials ought to have a unimodal distribution.

### 3 Neural Topographic Factor Analysis

NTFA extends TFA to model the range of variation across participants and stimuli. We assume exactly the same factor analysis model as TFA, which is to say that we model the fMRI signal as a linear combination of time-dependent weights and spatially varying Gaussian factors. NTFA additionally infers *embedding vectors* for individual participants and stimuli. We then learn a mapping from embeddings to the parameters of the likelihood model, parameterized by a neural network. This replaces the unimodal Gaussian hyperprior in HTFA with a deep generative model, and incorporates a mechanism for parameter sharing across trials.

We model  $N$  trials in which participants  $p_n \in \{1, \dots, P\}$  undergo a set of stimuli  $s_n \in \{1, \dots, S\}$  and are scanned for  $T$  time points per trial. We assume that participant embeddings  $\{z_1^p, \dots, z_P^p\}$  and stimulus embeddings  $\{z_1^s, \dots, z_S^s\}$  are shared across trials. For simplicity, we will consider the case where both embeddings have the same dimensionality  $D$  and

are distributed according to a Gaussian prior

$$z_p^p \sim \mathcal{N}(0, I), \quad z_s^s \sim \mathcal{N}(0, I). \quad (6)$$

For each participant  $p$ , we define the RBF center  $x_p^F$  and log-width  $\rho_p^F$  in terms of a neural mapping

$$x_p^F \sim \mathcal{N}(\mu_p^x, \sigma_p^x), \quad \mu_p^x, \sigma_p^x \leftarrow \eta_\theta^{F,x}(z_p^p), \quad (7)$$

$$\rho_p^F \sim \mathcal{N}(\mu_p^\rho, \sigma_p^\rho), \quad \mu_p^\rho, \sigma_p^\rho \leftarrow \eta_\theta^{F,\rho}(z_p^p). \quad (8)$$

Here  $\eta_\theta^F$  is a neural network parameterized by a set of weights  $\theta$ , which models how variations between participants and stimuli affect the factor positions and widths in brain activations. We similarly assume a neural network  $\eta_\theta^W(z_p^p, z_s^s)$  parameterizes the distribution over weights  $W_{n,t}$ , given the embeddings for each trial  $n$  and time point  $t$  with  $p = p_n, s = s_n$ :

$$W_{n,t} \sim \mathcal{N}(\mu_n^w, \sigma_n^w), \quad \mu_n^w, \sigma_n^w \leftarrow \eta_\theta^W(z_p^p, z_s^s). \quad (9)$$

The likelihood model is now the same as that in TFA,

$$Y_{n,t} \sim \mathcal{N}(W_{n,t} \cdot F_p, \sigma^Y), \quad F_p \leftarrow \kappa(x_p^F, \rho_p^F). \quad (10)$$

We summarize the generative model for NTFA in Algorithm 1. This model defines a joint density  $p_\theta(Y, W, x, \rho, z^p, z^s)$ , which in turn defines a posterior  $p_\theta(W, x, \rho, z^p, z^s | Y)$  when conditioned on  $Y$ . We ap-

---

**Algorithm 1** NeuralTFA Generative Model
 

---

$(p_1, \dots, p_N)$   $\triangleright$  Participant for each trial  
 $(s_1, \dots, s_N)$   $\triangleright$  Stimulus for each trial  
 1: **for**  $p$  **in**  $1, \dots, P$  **do**  
 2:  $z_p^p \sim \mathcal{N}(0, I)$   $\triangleright$  Equation (6)  
 3: **for**  $s$  **in**  $1, \dots, S$  **do**  
 4:  $z_s^s \sim \mathcal{N}(0, I)$   $\triangleright$  Equation (6)  
 5: **for**  $n$  **in**  $1, \dots, N$  **do**  
 6:  $p, s \leftarrow p_n, s_n$   
 7:  $(\mu_p^x, \sigma_p^x), (\mu_p^\rho, \sigma_p^\rho) \leftarrow \eta_\theta^F(z_p^p)$   
 8:  $x_p^F \sim \mathcal{N}(\mu_p^x, \sigma_p^x)$   $\triangleright$  Equation (7)  
 9:  $\rho_p^F \sim \mathcal{N}(\mu_p^\rho, \sigma_p^\rho)$   $\triangleright$  Equation (8)  
 10:  $\mu_n^W, \sigma_n^W \leftarrow \eta_\theta^W(z_p^p, z_s^s)$   $\triangleright$  Equation (9)  
 11: **for**  $t$  **in**  $1 \dots T$  **do**  
 12:  $W_{n,t} \sim \mathcal{N}(\mu_n^W, \sigma_n^W)$   $\triangleright$  Equation (9)  
 13:  $F_p \leftarrow \kappa(x_p^F, \rho_p^F)$   
 14:  $Y_{n,t} \sim \mathcal{N}(W_{n,t} \cdot F_p, \sigma^Y)$   $\triangleright$  Equation (10)

---

proximate the posterior with a variational distribution,

$$q_\lambda(W, \rho, x, z^P, z^S) = \prod_{n,t} q_{\lambda_{n,t}^W}(W_{n,t}) \prod_s q_{\lambda_s^S}(z_s^S) \prod_p q_{\lambda_p^X}(x_p^F) q_{\lambda_p^\rho}(\rho_p^F) q_{\lambda_p^Z}(z_p^p). \quad (11)$$

We learn the parameters  $\theta$  and  $\lambda$  by maximizing the evidence lower bound (ELBO)

$$\mathcal{L}(\theta, \lambda) = \mathbb{E}_q \left[ \log \frac{p_\theta(Y, W, x, \rho, z^P, z^S)}{q_\lambda(W, x, \rho, z^P, z^S)} \right] \leq \log p_\theta(Y).$$

As in all variational inference problems, the ELBO can be decomposed into a log-likelihood, which is sometimes known as the reconstruction loss, and a KL divergence, which acts as a regularizer,

$$\mathcal{L}(\theta, \lambda) = \mathbb{E}_q [\log p(Y | W, F, z^P, z^S)] - \text{KL}(q_\lambda || p_\theta).$$

For a software framework, we use Probabilistic Torch, a library for deep generative models that extends the PyTorch deep learning framework (Narayanaswamy et al., 2017). In lieu of the ELBO, we employ an importance-weighted bound (Burda et al., 2016) with a doubly-reparameterized gradient estimator (Tucker et al., 2019). This objective provides more accurate estimates for the gradient of the log marginal likelihood.

The advantage of incorporating neural networks into the generative model is that it enables us to explicitly reason about multimodal response distributions and effects that vary between individual samples. The network weights  $\theta$  are shared across trials, as are the stimulus and participant embeddings  $z_s^S$  and  $z_p^P$ . This allows NTFA to capture statistical regularities within a

whole experiment. At the same time, the use of neural networks ensures that differences in embeddings can be mapped onto a wide range of spatial and temporal responses. Whereas the hierarchical Gaussian priors in HTFA implicitly assume that response distributions are unimodal and uncorrelated across different factors  $k$ , the neural network in NTFA is able to model such correlations by jointly predicting all  $K$  factors.

While neural network models can have thousands or even millions of parameters, we emphasize that NTFA in fact has a *lower* number of trainable parameters than HTFA. TFA and HTFA assume fully-factorized variational distributions, requiring  $O(NK + NTK)$  learned parameters for  $N$  trials with  $T$  time points. In NTFA, the networks  $\eta^F$  and  $\eta^W$  will have  $O(D(D + K))$  parameters each, whereas the variational distribution will have  $O(D(P + S) + PK + NTK)$  parameters.

In practice, scanning time limitations impose a trade-off between  $N$  and  $T$  (the number of trials in a scanning run, and the length of a trial). For this reason  $NTK$  does not always dominate  $NK$ , since often  $T \propto O(10)$ . We can then choose  $D \propto O(1)$  and  $K \propto O(100)$ , and if we label constant factors  $c$ , the total number of parameters becomes  $O(cD^2 + cDK)$ , making  $O(cDK)$  the dominant term. NTFA can have orders of magnitude fewer parameters when  $D = 2$  as compared to HTFA.

## 4 Experiments

### 4.1 Datasets

We evaluate NTFA on four datasets. First, we verify that NTFA can recover a ground-truth embedding structure that, by construction, contains clearly distinguishable participant and stimulus clusters.

We present analysis of a previously unpublished in-house dataset, a pilot study pertaining to the subjective experience of fear. We present embedding results from these datasets analyzed without their resting-state trials. These experimental datasets vary in several qualities including the number of participants, time points, and voxels, and also task variables, testing how NTFA performs in a variety of experimental contexts.

Finally, we verify that NTFA can reconstruct the publicly available ‘‘Pie Man’’ dataset used to evaluate previous fMRI analysis models (Anderson et al., 2016). We consider a second publicly available dataset on emotional sounds and music, which contains many stimulus and participant categories (Lepping et al., 2016).

**Synthetic Data:** We consider a simulated dataset in which there are three participant groups of five participants each, which we call *Group 1*, *Group 2* and *Group 3*. All participants underwent two categories of hypo-

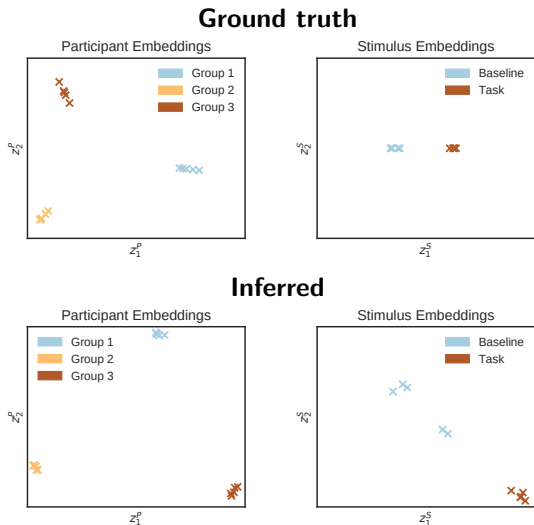


Figure 2: **Inferred embeddings for synthetic data:** We apply NTFA to a dataset in which three groups of participants exhibit varying levels of response in three different brain regions to *Task* and *Baseline* stimuli, depending on the ground truth locations of participant and stimulus embeddings (Top). Without prior knowledge of participant groups and stimulus categories, NTFA recovers these conditions as participant and stimulus embeddings (Bottom). Only the relative spatial arrangement is of interest.

thetical stimuli, called *Baseline* and *Task*, with five stimuli within each category. Each participant underwent a single hypothetical scanning run with rest trials interleaved between stimuli. We manually defined three distinct factors in a standard MNI\_152.8mm brain. We then sampled participant embeddings  $\{z_1^p, \dots, z_{15}^p\}$  and stimulus embeddings  $\{z_1^s, \dots, z_{10}^s\}$ , from mixtures of three and two distinct Gaussians respectively. We set the means for these Gaussians to meet the following conditions under noisy combination:

- All participants show no whole-brain response during rest besides random noise.
- Under *Baseline* stimuli, Group 1 exhibits half the response in the first region as compared to under *Task* stimuli, on average. The rest of the brain shows no response. Similarly, Group 2 and Group 3 exhibits a response in the second and third regions respectively, while the rest of the brain shows no response.
- Each *Baseline/Task* stimulus provokes a response lower or higher than the stimulus category’s average based on the stimulus embedding’s location.

**The Fear and Affective Videos (“AffVids”):** This is a dataset for a pilot study that we have carried out in-house. A total of 22 participants watched videos

Table 1: **Network architectures for  $\eta_\theta^F$  and  $\eta_\theta^W$**

Layer	$p_\theta(x_p^F, \rho_p^F   z_p^F)$	$p_\theta(W_{n,t}   z_p^F, z_s^S)$
Input	$z_p^F \in \mathbb{R}^D$	$z_p^F, z_s^S \in \mathbb{R}^D$
1	FC $D \times 2D$ PReLU	FC $2D \times 4D$ PReLU
2	FC $2D \times 4D$ PReLU	FC $4D \times 8D$ PReLU
3	FC $4D \times 8K$	FC $8D \times 2K$
Output	$(\mu_p^x, \sigma_p^x, \mu_p^\rho, \sigma_p^\rho) \in \mathbb{R}^{8K}$	$(\mu_n^w, \sigma_n^w) \in \mathbb{R}^{2K}$

Table 2: **Parameter counts:** When using low-dimensional embeddings, NTFA has roughly as many parameters as HTFA for the Pie Man dataset, and orders of magnitude fewer learnable parameters for other datasets, which have many more trials than participants ( $N \gg P$ ). We chose  $K = 100$  for both models across the real datasets, and  $D = 2$  for NTFA.

Dataset	HTFA parameters	NTFA parameters
Pie Man	$1.02 \times 10^7$	$1.02 \times 10^7$
Depression	$2.53 \times 10^7$	$2.61 \times 10^6$
AffVids	$1.64 \times 10^8$	$8.88 \times 10^6$
Synthetic ( $K = 3$ )	$2.16 \times 10^4$	$1.90 \times 10^4$

depicting fear-related content and rated affective and emotional impact after each clip. The stimuli consisted of 36 videos, separated into three fear-related content situations (spiders, heights, and social situations), each clip lasting 20 seconds. Participants provided subjective experience ratings (e.g. how much fear they felt) after each clip. The fMRI data contained 81,638 voxels and 1656 time points per scanning run.

**Emotional Musical and Nonmusical Stimuli in Depression (“Depression”)** (Lepping et al., 2016)<sup>1</sup>: 19 participants with major depressive disorder, and 20 control participants (N=39) underwent emotional musical and nonmusical stimuli to examine how neural processing of emotionally provocative auditory stimuli is altered within the anterior cingulate cortex and striatum in depression. The fMRI data had 353,600 voxels, and 105 time points for each scanning run. We refer to this dataset by the shorthand *Depression*, and show an example reconstruction from it in Figure 3.

**Pie Man Narrative Listening (“Pie Man”)** (Simony et al., 2016)<sup>2</sup>: In a between-subjects design, participants were assigned to one of four experimental stimulus categories that varied in the amount of structured narrative content that was presented. Participants either listened to an intact audio recording

<sup>1</sup>This data was obtained from the OpenfMRI database. Its accession number is ds000171.

<sup>2</sup><http://arks.princeton.edu/ark:/88435/dsp015d86p269k>

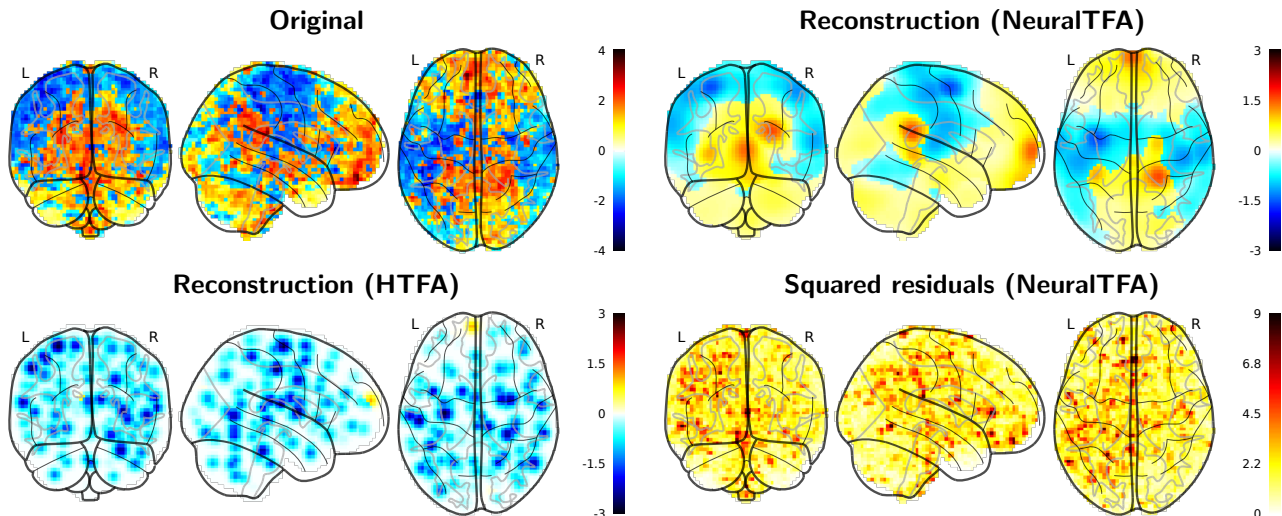


Figure 3: **Reconstructions for the Depression dataset:** We show images averaged across the TRs constituting a single trial, with a single participant and a single stimulus. The original image (top-left) enjoys a better reconstruction with  $K = 100$  by NTFA (top-right) than under HTFA (bottom-left). NTFA’s residuals (bottom-right) show that it captures detail across the brain rather than selectively reconstructing particular regions.

of the story *Pie Man* ( $N = 36$ ), or the same recording with paragraphs scrambled ( $N = 18$ ) or with words scrambled ( $N = 25$ ). A fourth group of participants were not presented with any recordings ( $N = 36$ ). The fMRI data had 61,367 voxels and 300 time points for each scanning run. The narrative was presented at a story-telling event organized by *The Moth*.

## 4.2 Training and Test Sets

We have split our datasets into training and test sets in a manner that ensures that the training set always contains at least one trial for each participant  $p \in \{1, \dots, P\}$  and each stimulus  $s \in \{1, \dots, S\}$ . To do so, we construct a matrix of  $(p, s) \in \{1, \dots, P\} \times \{1, \dots, S\}$  with participants as rows and stimuli as columns, choose its modulo-columns diagonals ( $\{(p, s) : p \bmod S = s\}$ ) as validation pairs. All blocks with these pairs of participant and stimulus belong to the test set; all others belong to the training set.

When maximizing the IWAE bound on the log evidence over the training set, we update all parameters  $\theta$  and  $\lambda$ . For our test set, we ran inference separately, adjusting only the single-trial (local) variational parameters  $\lambda_{n,t}^w$  for the trials  $n$  and time-points  $t$  having  $p_n$  and  $s_n$  such that  $p_n \bmod S = s_n$ . We update nothing else during inference on the test set.

The *Pie Man* experiment exposed many participants to only one stimulus, so we were unable to separate it into a training and test set. The other two real datasets provide data for each  $(p, s)$  of participant and stimulus,

and for these all results come from the test set.

## 4.3 Model Architecture and Training

We employ participant and stimulus embeddings of dimensions  $D = 2$  across our experiments for simplicity. For the synthetic dataset, we analyze the data with the same number of factors as were used to generate it,  $K = 3$ . For our experiments on real datasets, we employed  $K = 100$  factors to achieve good reconstruction performance without overfitting.

The network  $\eta_\theta^E(\cdot)$  is a multilayer perceptron (MLP) with 3 hidden layers and PReLU activations. We extract the factor parameters  $F, x$  and  $F, \rho$  from the appropriate dimensions of the  $8K$ -dimensional result. The network  $\eta_\theta^W(\cdot)$  is similarly an MLP with 3 hidden layers, though operating over both embeddings. We extract the weight parameters  $w_n$  from its  $2K$ -dimensional result. Architectural details for both networks are given in Table 1. The neural network weights  $\theta$  specify the linear layers of the networks.

We performed optimization using the Adam algorithm (Kingma and Ba, 2015), for 1000 epochs per dataset (including another 1000 on the local parameters of the test set), which was usually more than enough for the objective to converge. We used  $L = 100$  particles to calculate the log likelihood and the IWAE evidence bound. We report the number of parameters in our model, and in HTFA, in Table 2.

We used learning rates of  $1.0 \times 10^{-2}$  for the variational parameters  $\phi$  and  $1.0 \times 10^{-4}$  for the generative param-

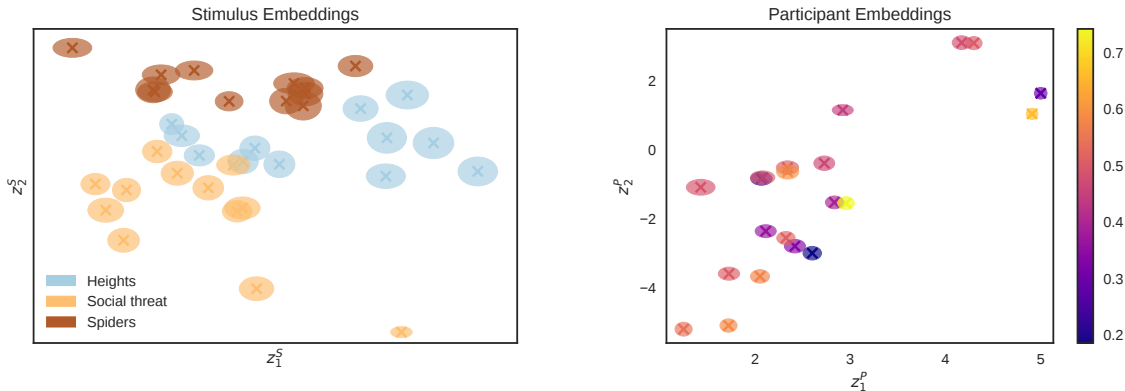


Figure 4: Participant and stimulus embeddings from the AffVids dataset. Crosses indicate the location of the (approximate) posterior mean, and ellipses display (approximate) posterior covariance. The labels are used only for visualization purposes. **Left:** Stimulus embeddings recovered groups of fear stimuli corresponding to heights, spiders, and social threats. The overlap may reflect intentionally low fear intensity on the part of the stimulus designers. **Right:** Participant embeddings are color-coded by their reported level of fear across all stimulus categories (heights, spiders, and social threats). Cooler colors indicate lower mean fear ratings, while warmer colors indicate higher mean fear ratings.

Table 3: **Model performance** in terms of log likelihood and log evidence. We approximate the log evidence with an importance-weighted estimator (Burda et al., 2016). For all datasets except Pie Man, we evaluate on a test set of held out subject-stimuli pairs. This is not possible for the Pie Man data, for which we report training set performance.

	HTFA	NTFA
<b>Log likelihood (Reconstruction Loss)</b>		
Synthetic ( $K=3$ )	$-4.69 \times 10^6$	<b><math>-4.68 \times 10^6</math></b>
AffVids	$-1.59 \times 10^8$	<b><math>-1.56 \times 10^8</math></b>
Depression	$-1.69 \times 10^8$	<b><math>-1.48 \times 10^8</math></b>
Pie Man*	$-5.01 \times 10^9$	<b><math>-4.36 \times 10^9</math></b>
<b>Log marginal likelihood (IWAE bound)</b>		
Synthetic ( $K=3$ )	$-4.72 \times 10^6$	<b><math>-4.68 \times 10^6</math></b>
AffVids	$-1.61 \times 10^8$	<b><math>-1.56 \times 10^8</math></b>
Depression	$-1.71 \times 10^8$	<b><math>-1.49 \times 10^8</math></b>
Pie Man*	$-5.24 \times 10^9$	<b><math>-4.38 \times 10^9</math></b>

ters  $\theta$ . We scheduled the learning rates with a patience of 100 epochs, and a multiplicative decline in learning rates (by 0.5 whenever learning rates were decreased). This only proved necessary when training NTFA on the synthetic dataset, for which 1000 epochs proved far more than needed for convergence.

## 5 Evaluation

We compare NTFA to HTFA in its reconstruction loss and the log marginal likelihood (a.k.a the model evidence). We report the log-likelihood (a.k.a. the

construction loss) and an importance-weighted bound to the log evidence for each dataset’s test set (except for Pie Man). We then examine the inferred embeddings for patterns based on stimulus categories, sorted participant categories, and individual differences.

Across datasets, NTFA exhibits a higher log-likelihood than the state-of-the-art model HTFA (Table 3), with the same number ( $K = 100$ ) of latent factors. Since our Synthetic dataset consisted of images generated solely from a limited number of factors and white noise, it offered the least performance gain in moving from HTFA to NTFA. In contrast, NTFA enjoys its greatest performance improvements in datasets like AffVids, in which the sharing of embeddings allows us to learn fine-grained individual stimulus representations while also reconstructing noisy data. We visualize an example reconstruction from the Depression dataset, on which NTFA also enjoyed substantial performance improvements over HTFA, in Figure 3.

**Synthetic Data:** For synthetic data, NTFA recovers stimulus and participant embeddings that are qualitatively very similar to the embeddings that we used to generate the data (Figure 2). We emphasize that embeddings are learned directly from the synthetic data in an entirely unsupervised manner, which means that there is in principle no reason that we would expect embeddings to be exactly the same. However, we do observe that learned embeddings for participants and stimuli are well-separated, appear to have some variance, and are invariant under linear transformations. Moreover, given the “true” number of factors ( $K = 3$ ), NTFA reconstructs synthetic data better than HTFA.

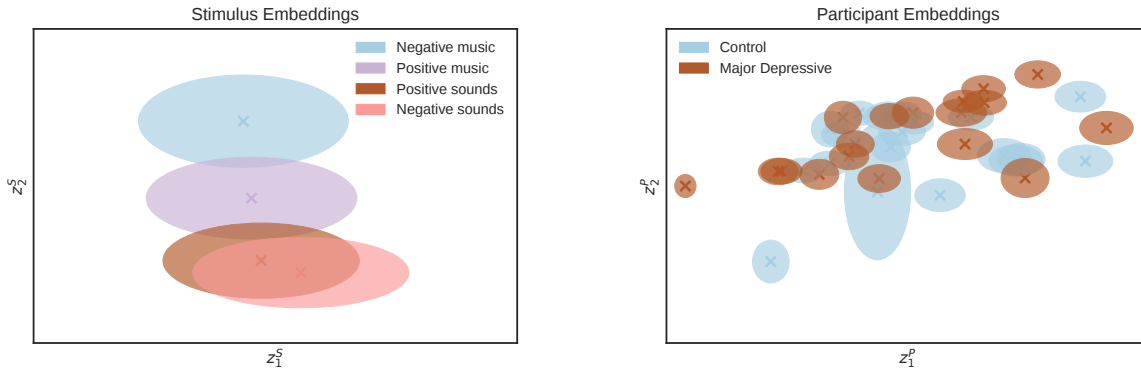


Figure 5: Participant and stimulus embeddings for the Depression dataset (Lepping et al., 2016). Crosses indicate the location of the variational mean, and ellipses display variational covariance. The labels are used only for visualization purposes. **Left:** Stimulus embeddings varied from tonal (top) to atonal (bottom). **Right:** Participant embeddings spanned from mostly depressed (lower-left) to mostly control (upper-right)

**Fear and Affective Videos dataset:** On the AfVids dataset, NTFA achieves better reconstructions than HTFA, as reported in Table 3. In an analysis without resting-state data, NTFA uncovered stimulus embeddings that clustered by category (Figure 4).

The participant embeddings do not seem to predict the self-reported fear ratings. However as shown in Figure 4 they do seem to uncover variations among participants in the latent space. Note, for example the participant groups breaking away from the central 'cluster' towards top-right and bottom-left. This suggests that there are factors not explained by the self-reported fear ratings that might be driving the individual variation in response among participants.

**Emotional Musical and Nonmusical Stimuli in Depression dataset:** On this dataset, NTFA similarly achieved better reconstruction loss than HTFA. The supplied metadata labeled stimuli by category rather than individually, so stimulus embeddings only acquired a linear gradation from tonal/musical to atonal/nonmusical. Participant embeddings for major depressive and control-group participants were closely scattered around a semi-apparent dividing line (Figure 5). Regularization could potentially separate the groups. We only labelled the embeddings for visualization; NTFA discovers this structure unsupervised.

**The “Pie Man” Narrative Listening dataset:** The Pie Man dataset (Simony et al., 2016) has previously been used to evaluate TFA and HTFA (Manning et al., 2018). Each participant underwent one trial with one stimulus in each scanning run, so only stimulus embeddings were shared across trials. NTFA did manage to improve over HTFA’s reconstruction loss on this

dataset, but it failed to disentangle meaningfully varied embeddings. We do not show its embedding plots.

## 6 Discussion

We have introduced Neural Topographic Factor Analysis (NTFA), an unsupervised model of spatio-temporal fMRI data which learns low-dimensional embeddings for participants and stimuli. We demonstrated that NTFA can recover ground-truth embedding clusters in synthetically generated data, and that it can reconstruct three datasets of real fMRI data better than the state-of-the-art using as few hidden factors as  $K = 100$ . NTFA attains higher log-likelihood than HTFA across data sets, for the same number of latent factors. When we set  $D = 2$ , NTFA learned embeddings from the real fMRI datasets that appeared to vary in a neuroscientifically meaningful way. This suggests that NTFA captures meaningful aspects of the underlying data.

Contrary to expectations of how a model can achieve superior reconstruction, NTFA requires fewer parameters. For the AfVids dataset, NTFA required on the order of 8.88 million parameters, as opposed to HTFA’s 164 million parameters, two orders of magnitude of advantage in compressing and representing large datasets. We see this advantage in datasets with many more trials than participants ( $N \gg P$ ), as shown in Table 2.

Neuroscientifically, the question remains open how efficiently factor analysis models such as TFA, HTFA, and NTFA actually compress data. The brain works on a many-to-many mapping from neural dynamics to observable psychological phenomena, with degeneracy at every level (Edelman and Gally, 2001; Marder and Taylor, 2011). Future studies of such methods could usefully consider how the reconstruction loss declines

as a function of the number of latent factors  $K$ . We arbitrarily fixed  $K = 100$ , while studies such as Manning et al. (2018) found optimal values as high as  $K = 700$  through cross-validation. Do such increases in parameterization lead to overfitting of fixed datasets, or can increasing NTFA’s model capacity lead to successful generalization on spatio-temporal neuroimaging data?

Practically, these techniques reflect a growing and urgent need for scalable analysis approaches in the neuroscience community. There are international efforts to collect fMRI datasets of hundreds or thousands of participants performing numerous cognitive tasks. Traditional analyses which do not efficiently compress the underlying data are not suited to guide inferences performed across such large samples. The approach we describe here ideally suits such datasets and offers the prospect to both clinicians and researchers of capturing meaningful, interpretable aspects of the data.

### Acknowledgments

The authors thank Jeremy Manning for insightful conversations. This work was supported by startup funds from Northeastern University, the Intel Corporation, the National Science Foundation (NCS 1835309), and the US Army Research Institute for the Behavioral and Social Sciences (ARI W911NF-16-1-0191).

### References

- Hervé Abdi and Lynne J. Williams. Principal component analysis. *Wiley interdisciplinary reviews: computational statistics*, 2(4):433–459, 2010.
- Michael J. Anderson, Mihai Capota, Javier S. Turek, Xia Zhu, Theodore L. Willke, Yida Wang, Po Hsuan Chen, Jeremy R. Manning, Peter J. Ramadge, and Kenneth A. Norman. Enabling factor analysis on thousand-subject neuroimaging datasets. *Proceedings - 2016 IEEE International Conference on Big Data, Big Data 2016*, pages 1151–1160, 2016. doi: 10.1109/BigData.2016.7840719.
- Yuri Burda, Roger Grosse, and Ruslan Salakhutdinov. Importance Weighted Autoencoders. In *International Conference on Learning Representations*, 2016. URL <http://arxiv.org/abs/1509.00519>.
- G. M. Edelman and J. A. Gally. Degeneracy and complexity in biological systems. *Proceedings of the National Academy of Sciences*, 98(24):13763–13768, 2001. ISSN 0027-8424. doi: 10.1073/pnas.231499798. URL <http://www.pnas.org/cgi/doi/10.1073/pnas.231499798>.
- Samuel J Gershman, David M Blei, Francisco Pereira, and Kenneth A Norman. A topographic latent source model for fmri data. *NeuroImage*, 57(1):89–100, 2011.
- James V. Haxby, J. Swaroop Guntupalli, Andrew C. Connolly, Yaroslav O. Halchenko, Bryan R. Conroy, M. Ida Gobbini, Michael Hanke, and Peter J. Ramadge. A common, high-dimensional model of the representational space in human ventral temporal cortex. *Neuron*, 72(2):404–416, 2011.
- Aapo Hyvärinen, Juha Karhunen, and Erkki Oja. *Independent Component Analysis*. Wiley Online Library, 2001.
- Diederik P. Kingma and Jimmy Ba. Adam: A Method for Stochastic Optimization. In *International Conference on Learning Representations*, pages 1–15, 2015. URL <http://arxiv.org/abs/1412.6980>.
- Rebecca J. Lepping, Ruth Ann Atchley, Evangelia Chryssikou, Laura E. Martin, Alicia A. Clair, Rick E. Ingram, W. Kyle Simmons, and Cary R. Savage. Neural processing of emotional musical and nonmusical stimuli in depression. *PLOS ONE*, 11(6):1–23, 06 2016. doi: 10.1371/journal.pone.0156859. URL <https://doi.org/10.1371/journal.pone.0156859>.
- Jeremy R. Manning, Rajesh Ranganath, Waitsang Keung, Nicholas B. Turk-Browne, Jonathan D. Cohen, Kenneth A. Norman, and David M. Blei. Hierarchical topographic factor analysis. In *Pattern Recognition in Neuroimaging, 2014 International Workshop On*, pages 1–4. IEEE, 2014a.
- Jeremy R. Manning, Rajesh Ranganath, Kenneth A. Norman, and David M. Blei. Topographic Factor Analysis: A Bayesian Model for Inferring Brain Networks from Neural Data. *PLOS ONE*, 9(5):e94914, May 2014b. ISSN 1932-6203. doi: 10.1371/journal.pone.0094914.
- Jeremy R Manning, Xia Zhu, Theodore L Willke, Rajesh Ranganath, Kimberly Stachenfeld, Uri Hasson, David M Blei, and Kenneth A Norman. A probabilistic approach to discovering dynamic full-brain functional connectivity patterns. *NeuroImage*, 2018.
- Eve Marder and Adam L Taylor. Multiple models to capture the variability in biological neurons and networks. *Nature neuroscience*, 14(2):133–138, 2011. ISSN 15378276. doi: 10.1016/j.dcn.2011.01.002.The.
- Siddharth Narayanaswamy, T. Brooks Paige, Jan-Willem van de Meent, Alban Desmaison, Noah Goodman, Pushmeet Kohli, Frank Wood, and Philip Torr. Learning Disentangled Representations with Semi-Supervised Deep Generative Models. In I. Guyon, U. V. Luxburg, S. Bengio, H. Wallach, R. Fergus, S. Vishwanathan, and R. Garnett, editors, *Advances in Neural Information Processing Systems 30*, pages 5927–5937. Curran Associates, Inc., 2017.
- Erez Simony, Christopher J Honey, Janice Chen, Olga Lositsky, Yaara Yeshurun, Ami Wiesel, and Uri Has-

son. Dynamic reconfiguration of the default mode network during narrative comprehension. *Nature communications*, 7:12141, 2016.

George Tucker, Dieterich Lawson, Shixiang Gu, and Chris J. Maddison. Doubly Reparameterized Gradient Estimators for Monte Carlo Objectives. In *International Conference on Learning Representations*, pages 1–12, 2019. URL <http://arxiv.org/abs/1810.04152>.